ACS Catalysis

pubs.acs.org/acscatalysis Research Article

Targeted Modification of Zeolites for Exceptionally Active and Selective Generation of PX and Light Olefins from Methanol−Toluene Co-Conversion

Yimo Wu, Nan Wang, Enze Chen, Haohao Feng, Dong Fan, Yang Yu, Li Wang, Te Ji, Zhengxi Yu, Jingfeng Han,* Yingxu Wei, and Zhongmin Liu*

Cite This: *ACS Catal.* 2025, 15, 4147−4159 Read Online

ACCESS | Metrics & More | Article Recommendations | Supporting Information

ABSTRACT: External surface modification is an effective means of achieving selective production in the acid-catalyzed process over the zeolite. However, catalyst modification, including external surface modification, often fails to break the seesaw effect between the reaction activity and selectivity. In the present work, an acid site-targeted chemical adsorption deposition (acid site-chemical adsorption−deposition (ASCAD)) method is applied to precisely control the deposition of silica. The modified ZSM-5 (ZSM-5-ASCAD) shows notable improvements in shape selectivity and catalytic activity in methanol−toluene coconversion. The total selectivity of light olefins and paraxylene (PX) reaches 94%, and the proportion of PX among xylene isomers is 99.5%. Meanwhile, toluene conversion is maintained at 43%, which is much higher than that over ZSM-5 modified by the conventional chemical liquid deposition (CLD) method (18%). Applying multiple techniques, including time of flight secondary ion mass spectrometry for depth profiling, the zero length column method combined with infrared microscopy (IRM) for diffusion evaluations and isotope labeling technology to reveal the mechanism and reaction pathway, we confirm that the ASCAD method achieves a minimized silica deposition that precisely shields the acid sites on the external surface while introducing only a slight impact on the diffusion compared to the severe diffusion depression of the CLD method. ASCAD modification effectively suppresses unwanted and uncontrollable side reactions and maintains high reactant conversion simultaneously. This unique modification method minimizes the disparity in mass transfer capability between the reactant methanol and toluene, which has not been achieved with other modification methods before, leading to enhanced methanol−toluene coconversion within the ZSM-5 crystal and exhibiting promoted ethene production and super high PX selectivity at the same time. Targeted modification of the zeolite surface provides an effective approach to simultaneously enhancing the activity and shape selectivity of zeolite-catalyzed reactions.

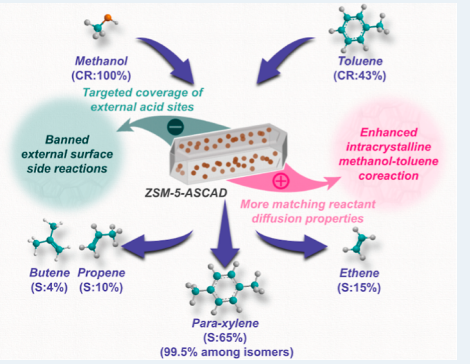

KEYWORDS: *heterogeneous catalysis, shape-selective catalysis, zeolites, catalyst modification, methanol−toluene coconversion*

INTRODUCTION

Paraxylene (PX) is a cornerstone raw material with a pivotal role in the industrial landscape and is often used as a monomer in the synthesis of purified terephthalic acid and further in the synthesis of industrial polymers such as polyethylene terephthalate (PET).[1] The current industrial production of PX is mainly based on petroleum as a raw material, obtained through the catalytic reforming of petroleum-based naphtha.[2] In contrast, applying methanol as an alternative carbon source from nonpetroleum resources in the coreaction with toluene is a reaction route with potential cost advantages and higher atomic utilization. Highly efficient coconversion of methanol with toluene for selective coproduction of PX and light olefins can be achieved via the adjustment of feed conditions and the modification of the catalyst, and it has been proved that toluene in the coreaction system leads the improved pathways for ethene production by introducing additional aromatic hydrocarbon pools, besides PX production.[3]

The unique acidic and cavity/channel structure of the zeolite brings about excellent catalytic performance. Cavity-type zeolite with small pore openings, such as the 8-membered ring, possesses an outstanding shape-selective effect on olefin products.[4] ZSM-5 with intersectional straight and sinusoidal 10-membered ring channels has acidity, hydrothermal stability, and suitable pore sizes close to the benzene ring diameter,[5] which makes it an ideal catalyst for the methanol−toluene

Received: December 17, 2024
Revised: January 24, 2025
Accepted: February 17, 2025

https://doi.org/10.1021/acscatal.4c07812
ACS Catal. 2025, 15, 4147−4159

Scheme 1. Deposition Process of TEOS with Different Adsorption Types and Comparison of Two Deposition Methods in the Present Study; (a) Physical Adsorption of TEOS and Thick Layer Deposition; (b) Chemical Adsorption of TEOS and Target Deposition; Here Take the Brønsted Acid Site as an Example; (c) Process of Conventional CLD Method. (d) Process of ASCAD Method Developed in the Present Study

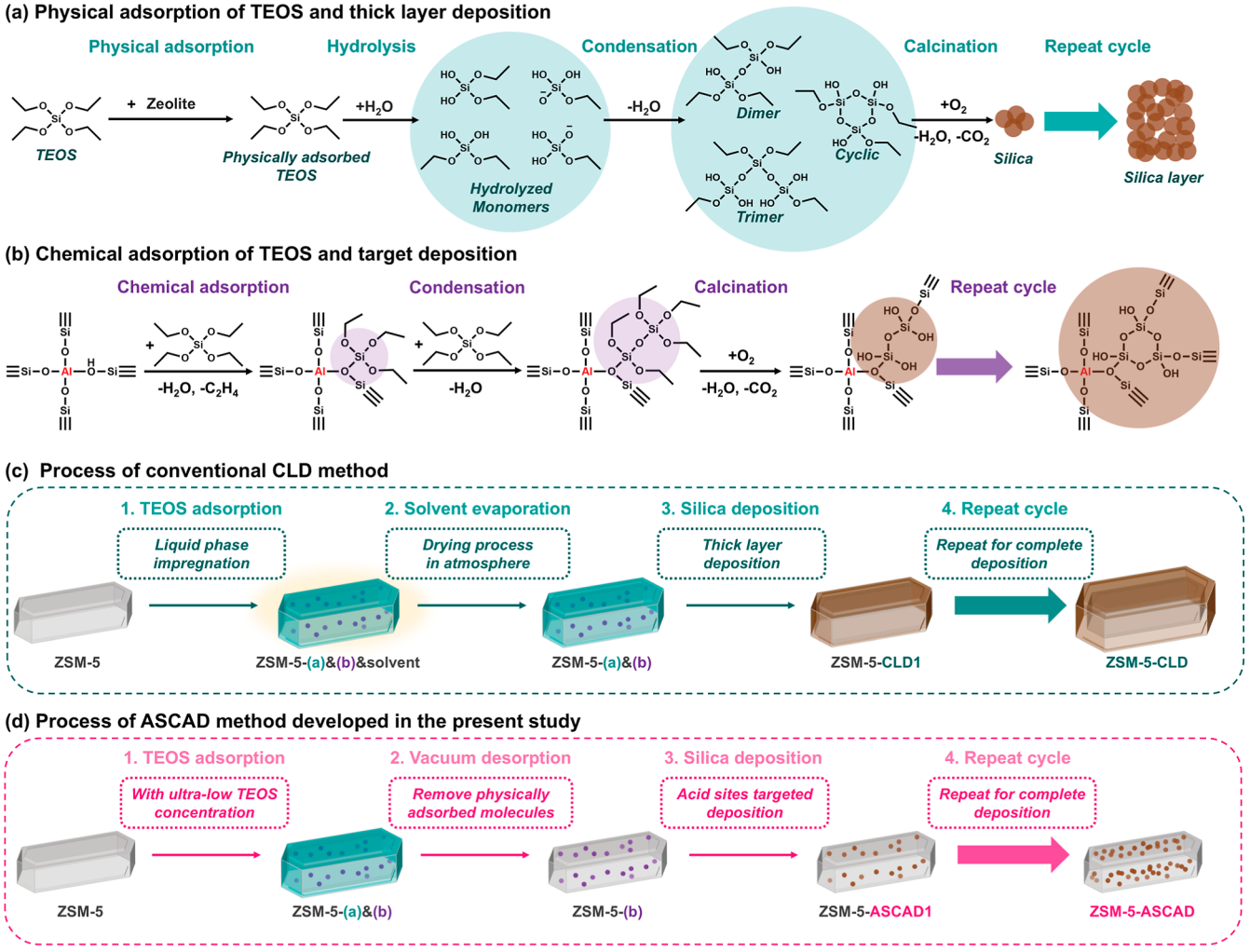

coreaction and a more promising catalyst for industrial applications. The critical issue for this reaction system is to suppress the reactions occurring on the external surface of ZSM-5 so that the coreaction can take place within the grain interior, thereby facilitating the shape-selective catalysis based on the topology and porosity of ZSM-5. Silica deposition, particularly through simple and inexpensive techniques, such as chemical vapor deposition (CVD) and chemical liquid deposition (CLD), is an effective strategy for shielding external acid sites.[6,7] Although there were many reports on the silica deposition method,[8−14] compared to some other means of zeolite modification and preparation, e.g., the epitaxial growth of a silicalite-1 layer over ZSM-5 crystal,[15] and selective exposure of the sinusoidal channel of the ZSM-5,[16] the current results of silica deposition method have not achieved ultrahigh PX selectivity (over 99%) and high reactant conversion activity as the methods mentioned above. It is imperative to develop more precise and efficient silicon oxide deposition approaches to innovate catalyst modification strategies for a more efficient and shape-selective process.

The deposition process of silica using tetraethyl orthosilicate (TEOS) as the silicon source goes through adsorption, hydrolysis, condensation, calcination, and other steps.[17] The deposition process of TEOS with different adsorption types is given in Scheme 1a,b. For physically adsorbed TEOS, under the promotion of water, silanol groups are formed by the self-hydrolysis of TEOS and create siloxane bridges through condensation reactions. Silica is generated by the dehydration condensation reaction in the oxidation process and further growth to form a silica layer in repeated cycles (see Scheme 1a).[18] On the external surface of zeolite, TEOS molecules preferentially interact with accessible acid sites, e.g., the bridging hydroxyl groups (see Scheme 1b). Hydroxyl groups partially condense with vicinal silanol groups to form Si−O−Si bonds during the calcination process.[17] Both physical adsorption and chemical adsorption of TEOS would take place in the CLD and CVD processes. The difference between the two processes is that, in the context of the CLD process, due to the sufficient water supply in the atmosphere air, a large amount of TEOS forms silicon-based compounds through self-hydrolysis and condensation. The silicon-based polymers grow and further condense with the hydroxyl groups on the external surface of the zeolite to form a thick silica deposition layer (see Scheme 1c). In the context of the CVD process, TEOS is carried by inert gas with a significantly reduced water content and preferentially chemically adsorbed at the acid sites. Even so, the generated

https://doi.org/10.1021/acscatal.4c07812
ACS Catal. 2025, 15, 4147−4159

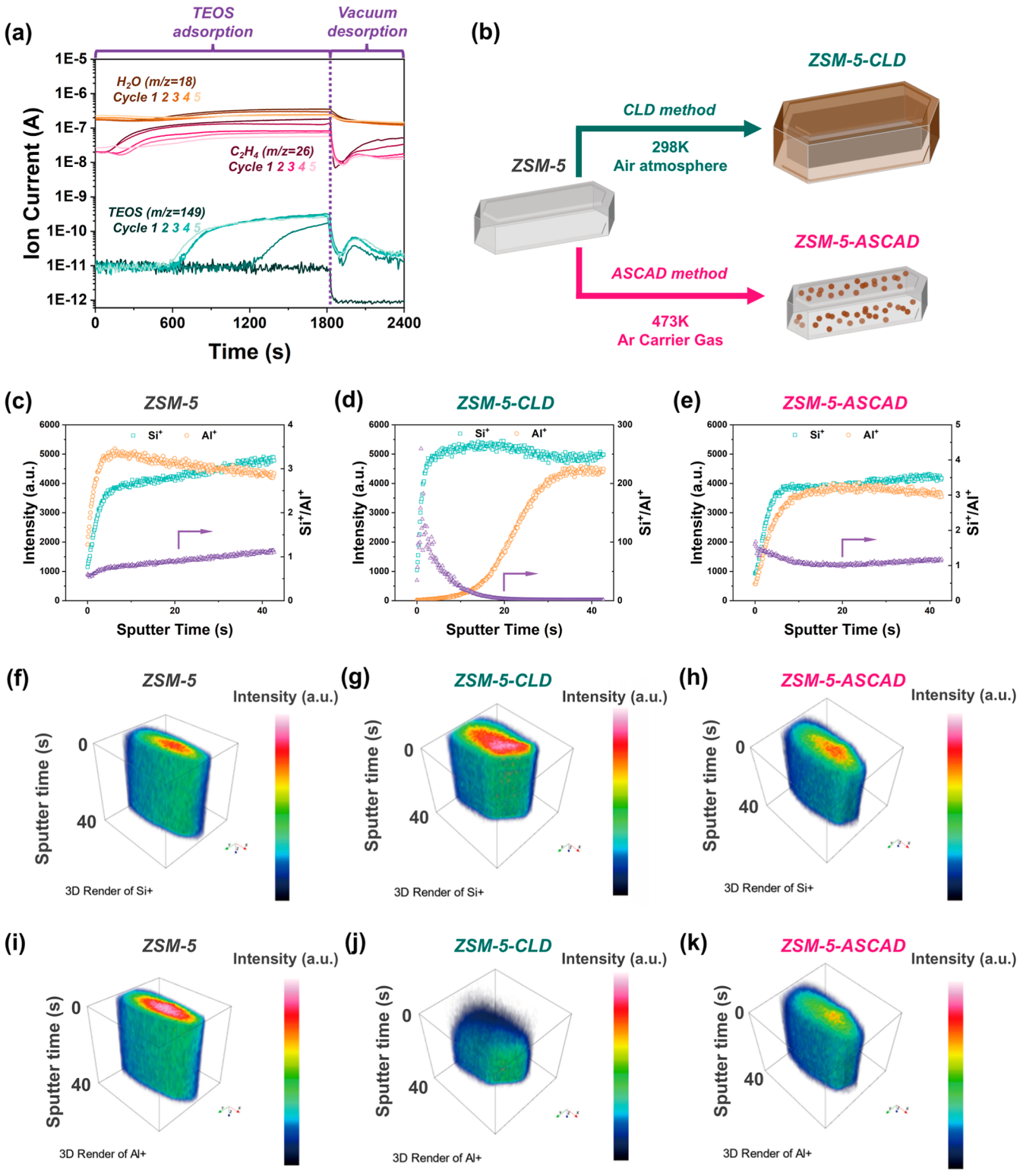

Figure 1. Different deposition effects exhibited in the CLD method and the ASCAD method. (a) Online mass spectrometry of multiple ASCAD cycles. (b) Sketch map of the CLD and the ASCAD deposition processes. (c–e) Depth profiles of Si and Al secondary-ion fragments contained in the sputtered volume at the upper surface layer measured by TOF-SIMS. Note that the obtained ratio is not an atomic Si/Al ratio but merely the Si^+/Al^+ secondary ion ratio. (f–h) TOF-SIMS 3D visualization of the spital distribution of Si secondary-ion fragments as a function of sputter time. (i–k) TOF-SIMS 3D visualization of the spital distribution of Al secondary-ion fragments as a function of sputter time.

water in the chemical adsorption process also drives the self-hydrolysis of a fraction of physically adsorbed TEOS to form silicon-based compounds, which cannot be completely removed by purging and would further form undesired nontarget silica deposition. Essentially, the CVD and CLD methods share similarities, as they are modification processes in which physical and chemical adsorption deposition coexist. The difference lies in the amount of silica deposition.

https://doi.org/10.1021/acscatal.4c07812
ACS Catal. 2025, 15, 4147–4159

In this study, an acid site-chemical adsorption−deposition (ASCAD) method (see Scheme 1d) is employed in the zeolite modification, by applying ultralow concentration of TEOS feeding gas in the adsorption process, and a following vacuum desorption process to remove the physical-adsorbed TEOS to prevent the formation of self-hydrolyzed silicon-based polymers. The ASCAD method developed in this paper can effectively remove physically adsorbed silicon sources and their hydrolysis products, achieving a separate chemical adsorption deposition process and targeted deposition on the external surface acid sites of the zeolite. To provide a more differentiated presentation of physical adsorption deposition versus separate chemical adsorption deposition, we conducted a comparative study on ZSM-5-CLD and ZSM-5-ASCAD catalysts. Compared with catalysts with other modification methods, the modified ZSM-5-ASCAD shows exceptional shape selectivity and catalytic activity in methanol−toluene coconversion, realizing highly efficient coproduction of PX and light olefins in a single catalysis process. Furthermore, the coupling of diffusion and reaction is a typical feature of zeolite catalysis, and diffusion behavior in zeolites is a key factor in determining the catalytic performance. In this study, multiple techniques are applied to investigate the diffusion properties and reaction pathway changes before and after modification, and to reveal how the modification with the ASCAD method leads to excellent catalytic performance.

METHODS

Catalyst Preparation. ZSM-5 (Si/Al = 67) was purchased from the Catalyst Plant of Nankai University and was calcined in flowing air at 823 K for 4 h to remove the template, and then was extruded and sieved into small particles in 40−60 meshes. Modification of ZSM-5 by the CLD method was carried out with tetraethyl orthosilicate (TEOS) as a silicon source. TEOS solution in cyclohexane with a concentration of 0.5 mol/L was prepared. 500 mg of catalyst to be treated was placed in a crucible and dried at 393 K for 12 h. After being cooled to 303 K, 0.5 mL of TEOS solution was added with a pipet gun. The impregnation process was continued for 12 h and repeated one time. The treated catalyst was calcined in a tube furnace in flow air at 823 K for 4 h. The obtained catalyst was named ZSM-5-CLD.

Modification of ZSM-5 by the ASCAD method also used TEOS as the silicon source. The ASCAD method was performed in a tube furnace. The loaded catalyst was pretreated at 773 K in flowing argon gas for 4 h to remove impurities. After cooling to 473 K, the TEOS saturated at 287 K (114 Pa) was carried into the tubular with a constant flow rate (20 mL/min) of argon gas for 30 min. The vacuum desorption process was then carried out by closing the inlet valve and turning the outlet to a Pfaff diaphragm pump. The vacuum process was maintained for 10 min to remove the excess physisorbed TEOS. The effluents of the TEOS adsorption process and vacuum desorption process were collected and detected by mass spectrometry. Finally, the catalyst was calcined at 823 K under flowing air (100 mL/min) for 30 min to remove the organic residues adsorbed on the catalyst and to deposit silica on the external surface of the zeolite. The above operation was repeated five times, and the treated catalyst was named ZSM-5-ASCAD.

Catalyst Test. Coreaction of methanol with toluene was performed in a fixed-bed quartz tubular reactor (inner diameter 4 mm) under atmospheric pressure. 50 mg of catalyst was loaded into the reactor and activated in argon flow at 823 K and then adjusted to the reaction temperature (733 K). The reactants were fed by passing the carrier gas (Ar) through the saturators maintained at 287 K. Molar ratios of methanol to toluene (M/T = 2) were obtained by adjusting the flow rates of the carrier gas. The total weight hourly space velocity (WHSV) of the reactants was maintained at 2 h^{-1} for different feed ratios. The effluent with a time on stream (TOS) of 20 min was collected and analyzed by gas chromatography (Agilent 7890B with flame ionization detector).

The calculation method of methanol−toluene coreaction was similar to our previous study.[3] The definitions of the molar conversion of methanol (C_M) and toluene (C_T) were as follows

$$C_M\ (\%) = \left(1 - \frac{M_{MeOH} + M_{DME}}{M \times \frac{r}{r+7}}\right) \times 100 \quad (1)$$

$$C_T\ (\%) = \left(1 - \frac{M_T}{M \times \frac{7}{r+7}}\right) \times 100 \quad (2)$$

where r represents the feed molar ratio of methanol to toluene; M_{MeOH}, M_{DME}, and M_T correspond to the carbon molar proportion of methanol, dimethyl ether, and toluene in the effluent, respectively; and M represents the sum of the carbon molar proportion of all the effluents.

And the conversion of the carbon resource was defined by

$$C\ (\%) = \left(1 - \frac{M_{MeOH} + M_{DME} + M_T}{M}\right) \times 100 \quad (3)$$

The selectivity of product I was defined by

$$S_I\ (\%) = \frac{M_I}{M - M_{MeOH} - M_{DME} - M_T} \times 100 \quad (4)$$

And the carbon resource utilization efficiency was defined by

$$U\ (\%) = C\ (\%) \times (S_{PX} + S_{C_2H_4} + S_{C_3H_6} + S_{C_4H_8})(\%) \div 100 \quad (5)$$

RESULTS AND DISCUSSION

Catalyst Characterization. The online mass spectrometry of multiple ASCAD cycles (see Figure 1a) shows that, for the first ASCAD cycle, there is no TEOS signal (selected m/z = 193, TEOS fragment with the highest relative intensity) in the adsorption stage, which indicates that TEOS is completely adsorbed. A TEOS signal is detected after 1200 s in cycle 2 and appears earlier as cycle times increase, and also the signal intensity of ethene (selected m/z = 26) and H_2O (selected m/z = 18) becomes lower, both of which indicate that the acid sites are covered gradually. The tailed peak of TEOS at about 2100 s in the vacuuming desorption stage indicates that the physisorbed TEOS is effectively removed, which ensures that there is no excess silica deposition. The sketch map of the two deposition processes is given in Figure 1b based on the SEM images of the catalyst samples (see Figure S1). The structural properties of ZSM-5 and surface-modified ZSM-5 are listed in Table S1. After the silica deposition on the external surface, the Si/Al ratio of the samples increases, while the decrease in the specific surface area and micropore volume depends on the modification method. It is worth noting that the ASCAD method only causes a slight variation in the Si/Al ratio and surface area, implying a low Si deposition amount and the surface area and pore volume of the zeolite being well-kept. In

https://doi.org/10.1021/acscatal.4c07812
ACS Catal. 2025, 15, 4147−4159

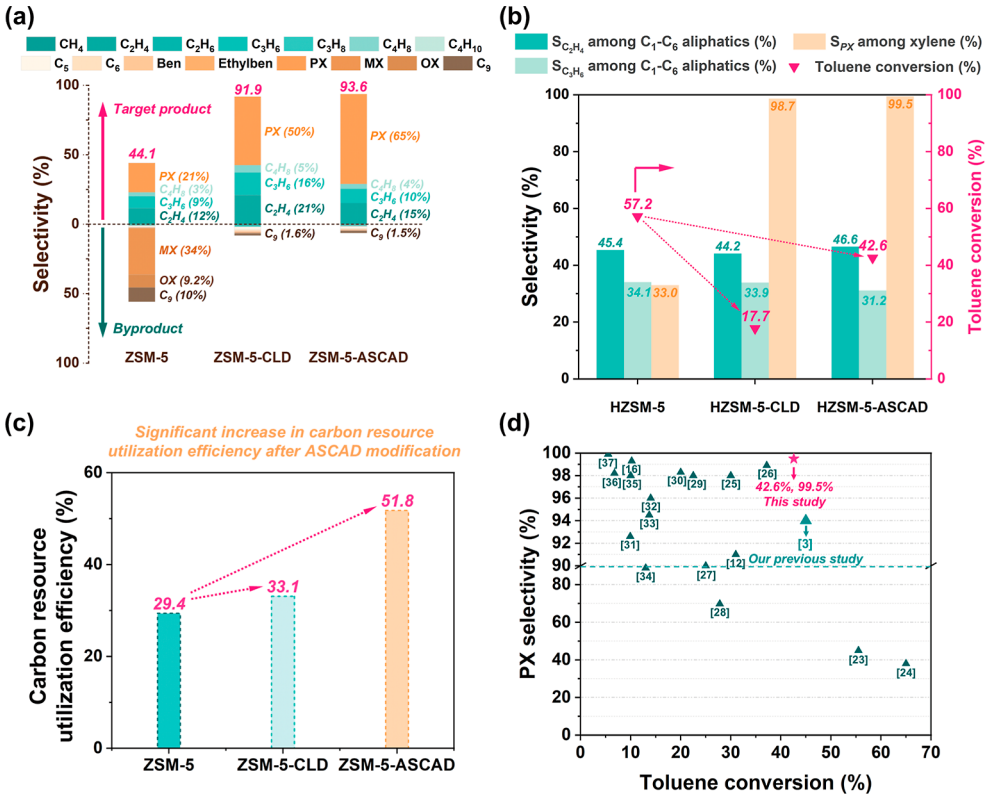

Figure 2. Catalytic performance of ZSM-5 and surface-modified ZSM-5. (a) Product selectivity of coreaction of methanol and toluene over the three catalysts. Feed ratio: $M/T = 2$, catalysts weight: 50 mg, WHSV: 2 h^{-1}, reaction temperature: 733 K, atmosphere pressure, TOS: 20 min. (b) Crucial performance indicators: toluene conversion and target product selectivity. (c) Carbon resource utilization efficiency of the coreaction: conversion efficiency of methanol and toluene into target products of PX and light olefins. (d) Comparison of PX selectivity and toluene conversion of ZSM-5-ASCAD with the catalysts in the literature and our previous study.

addition, all of the samples possess good crystallinity (see Figure S2) and low acid density (see Table S2). Compared with ZSM-5-CLD, the thickness of the silica deposition layer is greatly reduced over ZSM-5-ASCAD, which can be further confirmed by depth profiling of the zeolite external surface.

Time of flight secondary ion mass spectrometry (TOF-SIMS) sputter depth profiling of zeolite crystals can yield valuable surface specific chemical information based on the detected fragment ion composition.[19,20] Here, the TOF-SIMS sputter depth profiling of the catalyst surface layer complements the direct evidence of the presumed above sketch map. For ZSM-5-CLD, the intensity of the surface Si secondary-ion fragments is significantly higher than that of ZSM-5, and there is an aluminum-free layer over the external surface (see Figure 1c,d). However, for ZSM-5-ASCAD, depth profiles of Si and Al secondary-ion fragments contained in the sputtered volume at the upper surface layer are similar to that of ZSM-5 but with a lower Al content, implying that the targeted silica deposition over acid sites has been successfully achieved (see Figure 1c,e). TOF-SIMS 3D visualizations of the spital distribution of Si and Al secondary-ion fragments give a more intuitive display of the surface sputtering layers of the three zeolites (see Figure 1f–h for Si^+, and Figure 1i–k for Al^+). Comparing the surface sputtering layers of ZSM-5 and ZSM-5-CLD, it indicates that a thicker silica deposition layer is formed on the external surface of ZSM-5 zeolite after modification by the CLD method, and the thickness of the silica deposition layer is recorded by scanning transmission electron microscopy (STEM) images of the cross-section of ZSM-5-CLD obtained by the focused ion beam (FIB) (see Figure S3). The amorphous silica layer on the external surface of ZSM-5-CLD is significantly different from the bulk phase MFI structure, which may seriously affect the diffusion of reactants and products, and even cause the complete blockage of zeolite pores. In contrast, silica is preferentially deposited around the external surface acid sites of the zeolite after modification by the ASCAD method, retaining the original external surface of the zeolite to the greatest extent. This precise control of silica deposition may avoid the strong diffusion restriction for the reactant toluene.

Methanol–Toluene Co-Conversion Test. Due to the precise control of the deposition amount of silica and effective removal of physical adsorption deposition, the selectivity of PX in xylene increases significantly with the increase of ASCAD cycles (see Figure S4 and Table S3). At the same time, the loss of toluene conversion is significantly reduced (see Figure S4 and Table S4, and a comparison with the CVD method is also provided). What is more, the difference in the surface structure and composition of the three catalysts (ZSM-5, ZSM-5-CLD, and ZSM-5-ASCAD) is directly reflected in the catalytic performance. Olefins and aromatics are the main products in the coreaction of methanol with toluene. Surface modification of the zeolite contributes to combined strategies of reaction pathway guidance and zeolite shape-selective catalysis, which ensure high selective production of target products including PX and light olefins.[3] As shown in Figure 2a and Table S5, the total selectivity of PX and light olefins has been increased from less than 50% to more than 90% after external surface modification, which indicates that both the two external surface modification

https://doi.org/10.1021/acscatal.4c07812
ACS Catal. 2025, 15, 4147–4159

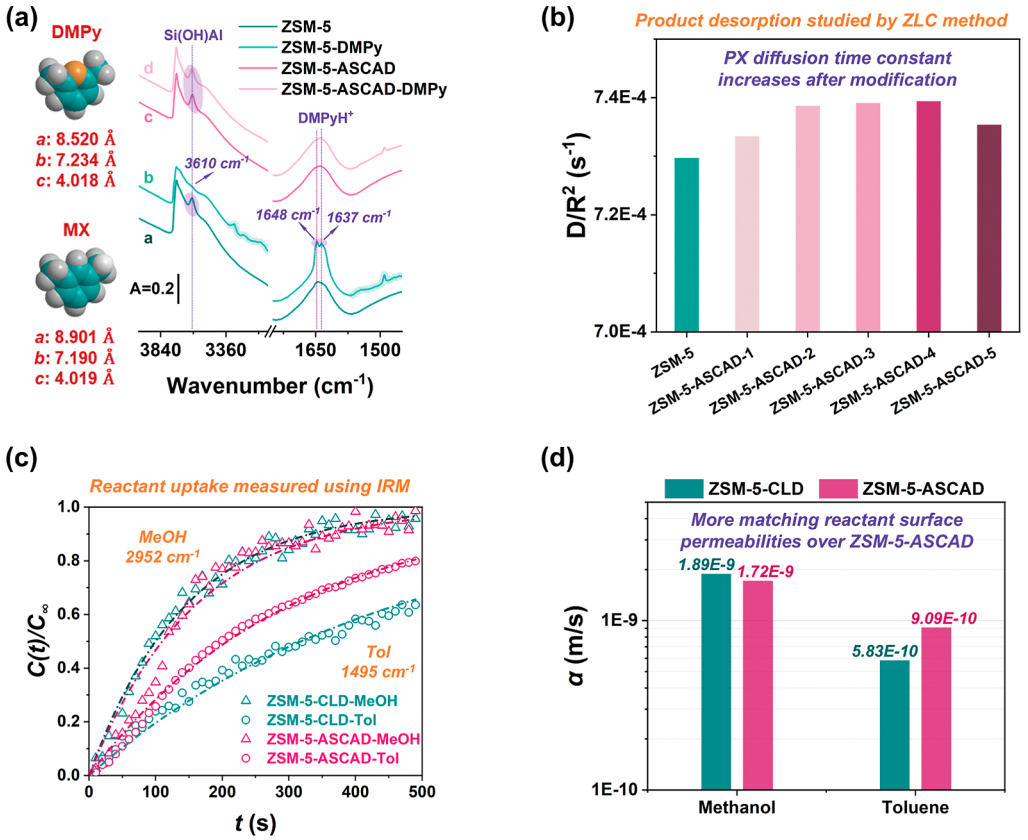

Figure 3. Acidity and diffusion properties. (a) Infrared spectra of the ZSM-5 and ZSM-5-ASCAD before and after 2,6-dimethylpyridine (DMPy) adsorption. Adsorption temperature: 373 K, desorption temperature: 423 K. (b) PX diffusion time constants (D/R^2) with ASCAD cycles studied by the ZLC method. (c) Integral uptake curves of the reactant on ZSM-5-CLD and ZSM-5-ASCAD measured using IRM. (d) Surface permeability (α) of the reactant on ZSM-5-CLD and ZSM-5-ASCAD obtained from fitting the surface-barrier-limited equation on uptake curves.

methods effectively inhibit the formation of byproducts and realize the adjustment of the product distribution, making light olefins and PX the main products of the methanol−toluene coreaction system. The difference is that ZSM-5-ASCAD has the advantage in PX selectivity among all products (65 vs 50%) and also in the total selectivity of light olefins and PX (93.6 vs 91.9%) compared with ZSM-5-CLD (see Figure 2a).

The ethene selectivity among C_1 to C_6 chain hydrocarbons is slightly different with the order of ZSM-5-ASCAD (46.6%) > ZSM-5 (45.4%) > ZSM-5-CLD (44.2%) (see Figure 2b). The advantage in the selectivity of PX (65%) and ethene (46.6% among C_1 to C_6) over ZSM-5-ASCAD indicates that more toluene may participate in methanol−toluene coconversion for optimized PX and ethene production.[21] Another significant superiority of ZSM-5-ASCAD is its stronger shape-selectivity on xylene isomers (S_{PX} = 99.5% among xylene isomers, see Figure 2b). Due to the close boiling points of the xylene isomer, it is unpractical to separate them through distillation.[5] The separation process used in industry such as crystallization needs massive energy consumption for deep cooling.[22] Thus, the increase in the selectivity of PX among xylene isomers (99.5% over ZSM-5-ASCAD vs 98.7% over ZSM-5-CLD) means a significant cost reduction. More importantly, ZSM-5-ASCAD also has a notable advantage over ZSM-5-CLD in toluene conversion (42.6 vs 17.7%, see Figure 2b). Generally, it is difficult to achieve both high PX selectivity and a high toluene conversion rate through surface modification. The increase in the catalytic activity of the reactant toluene and selective production of PX and light olefins would remarkably improve the process economy. Thus, compared with the conventional silica deposition method of CLD, by the precise control of silica deposition with the ASCAD method, both selectivity and activity advantage have been achieved over ZSM-5-ASCAD. Furthermore, carbon resource utilization efficiency, i.e., the conversion efficiency of methanol and toluene into target PX and light olefins, is defined to evaluate the catalytic performance differences in methanol−toluene coreaction over the three catalysts (see Figure 2c). The improvement of carbon source utilization efficiency is more significant after ASCAD modification compared with the CLD modification (from 29.4 to 51.8% for ASCAD modification and 33.1% for CLD modification). Although target product selectivity has been successfully improved by the CLD method, methanol−toluene coreaction over ZSM-5-CLD with low toluene conversion has not broken the seesaw effect between selectivity and reaction activity to achieve high carbon resource utilization efficiency. In contrast, high reactant conversion and high target product selectivity jointly lead to significantly improved carbon resource utilization efficiency over ZSM-5-ASCAD. When comparing methanol−toluene coreaction results with the works published in the literature, which utilize various other modification methods, the ZSM-5-ASCAD developed in our current study demonstrates outstanding advantages in terms of PX selectivity and toluene conversion (see Figure 2d and Table S6).[3,12,16,23−37] Besides, the methanol−toluene coreaction process in the present work, while producing PX, simultaneously enables the generation of light olefins (particularly enhancing the production of ethene), offering a new scheme for the

https://doi.org/10.1021/acscatal.4c07812
ACS Catal. 2025, 15, 4147−4159

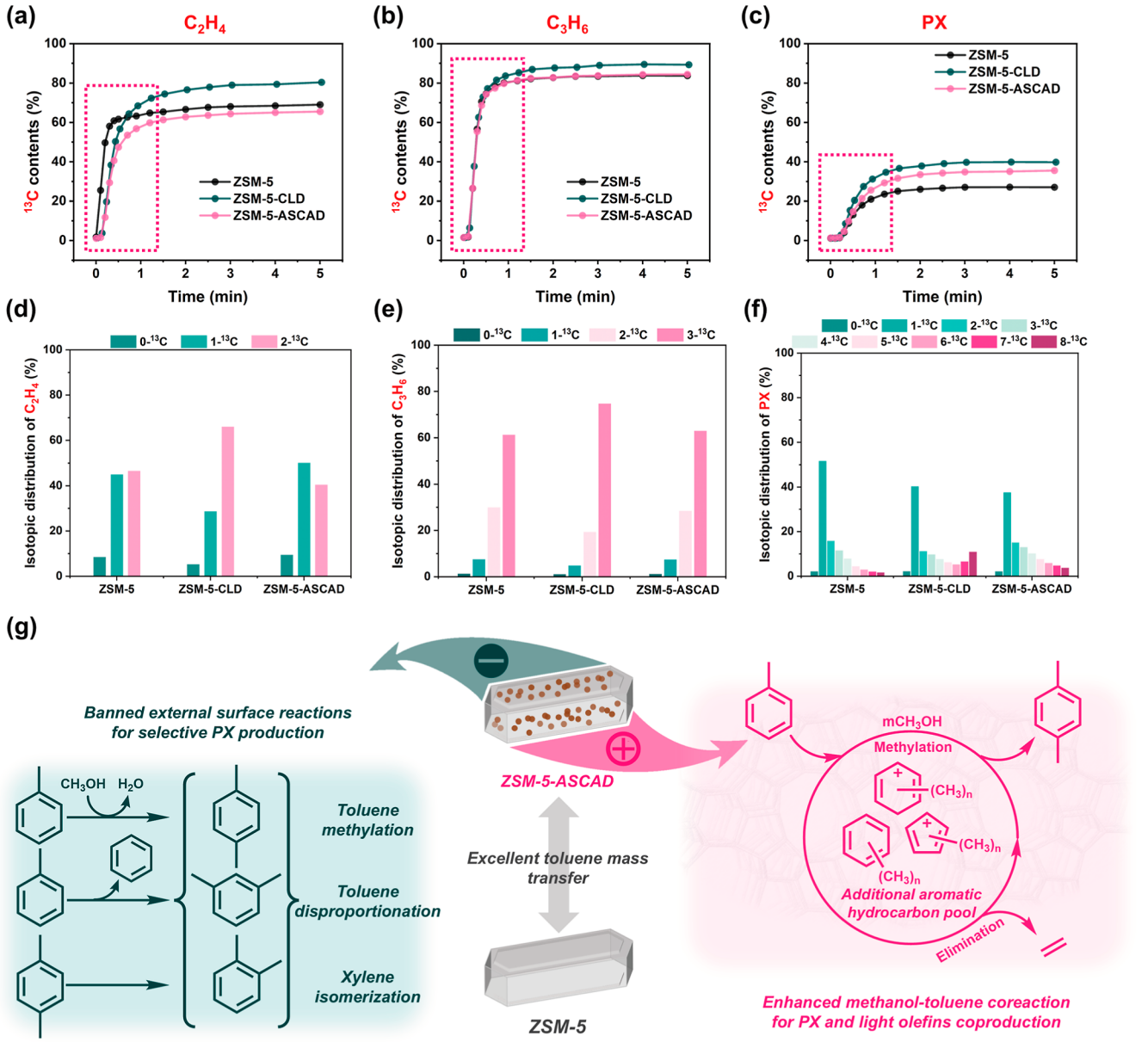

Figure 4. Isotope switching experiments revealing the reaction pathway change after surface modification. (a–c) ^{13}C contents of ethene (a), propene (b), and PX (c) after $^{12}C/^{13}C$-methanol switching. Feed ratio: M/T = 2. Catalysts weight: 50 mg, WHSV: 2 h^{-1}, reaction temperature: 733 K, atmosphere pressure, TOS: 20 min, time after switching: 5 min. (d–f) Isotopic distributions of ethene (d), propene (e), and PX (f) of 5 min after ^{13}C switching. (g) Reaction pathway change after surface modification by the ASCAD method.

production of basic chemical raw materials for the manufacture of PET.[38]

Catalyst Acidity and Diffusion Properties. Infrared spectroscopy of adsorbed 2,6-ditertbutylpyridine (DTBPy) is employed to characterize the external acid properties of zeolite.[39−41] As shown in Figure S5, the intensity reduction of the IR band of adsorbed DTBPy suggests that the external surface acid sites are significantly reduced after surface modification. Another probe molecule, 2,6-dimethylpyridine (2,6-DMPy), whose molecular size is close to that of meta-xylene, was also used to study the acidity properties of ZSM-5 and ZSM-5-ASCAD and possible inhibition of the reaction by external acidic catalysis (see Figure 3a). For ZSM-5, the broad peak at 3610 cm^{-1}, attributed to the bridging hydroxyl species, almost disappears after DMPy desorption at 423 K, and $DMPyH^+$, the protonated form of DMPy from the combination of DMPy with the Brønsted acid sites, appears at 1648 and 1637 cm^{-1}, which indicates that DMPy, especially some small-sized isomers of DMPy with para substitution, can enter the ZSM-5 grain and occupy the Brønsted acid sites of both the external surface and the internal channel.[42] In contrast, on ZSM-5-ASCAD, there is no significant change in the IR absorbances before and after DMPy adsorption. This indicates that, first, the ASCAD method has achieved successful coverage of the acidic sites on the external surface, and second, 2,6-DMPy cannot enter the ZSM-5-ASCAD grain, since the external surface isomerization reaction is inhibited after ZSM-5 is modified by ASCAD method, and the 2,6-DMPy molecule with a size close to meta-xylene is difficult to enter the ZSM-5-ASCAD grain, while the acid sites in the channel of ZSM-5 without modification are accessible for the isomerized DMPy with para substitution generated with the catalysis from external acidity.

https://doi.org/10.1021/acscatal.4c07812
ACS Catal. 2025, 15, 4147−4159

Further, PX diffusion time constants (D/R^2) in ZSM-5 modified by the ASCAD method with 1−5 cycles are measured by the zero-length column (ZLC) method and given in Figures 3b and S6. Note that the diffusion time constant of PX after ASCAD modification is slightly increased from the first to fourth cycle. Therefore, besides shielding the acid sites on the external surface to avoid the side reactions to produce xylene isomers and C_9 aromatics, the ASCAD modification method is beneficial to the diffusion of the product PX into the gas phase effluent, both of which directly contribute to the ultrahigh PX selectivity in the coreaction of methanol with toluene.

The diffusion behavior of reactant molecules imposes prominent effects on their apparent reactivity.[43] For the methanol−toluene coconversion system, the difference in the mass transfer efficiency between methanol and toluene significantly affects the reaction pathways.[44] In addition, the energy barrier difference between the intracrystalline diffusion and isomerization of xylene isomers directly determines the para-selectivity of the xylene products.[45] Infrared microscopy (IRM) has been developed to monitor the mass transfer of guest molecules on a particular nanoporous crystal.[46] By using the normalized areas of the IR bands of the adsorbates to quantify their relative concentrations in the zeolites (see Figure S7), the molecular uptake curves can be recorded for the investigation of adsorption kinetics (see Figure S8).[47] In the present study, we use IRM to measure multiple-crystal integral uptake curves of the reactant methanol and toluene (see Figure 3c), IR bands of methanol at 2952 cm^{-1} and toluene at 1495 cm^{-1} are used to plot the uptake curves,[48,49] and the surface permeability (α) of the reactants is obtained by fitting surface-barrier-limited equation on uptake curves.[50] As shown in Figure 3d, the α of methanol on ZSM-5-CLD is slightly higher than that on ZSM-5-ASCAD, while the α of toluene on ZSM-5-ASCAD is about two times higher than that on ZSM-5-CLD. Surface modification of zeolites allows selectively enhancing or depressing of the mass transfer of guest molecules depending on their molecular size and polarity.[51] Since the molecular size of methanol is distinctly smaller than the pore diameter of ZSM-5, the thick silica deposition layer formed by the CLD method increases the surface permeability of methanol instead of causing a stronger diffusion limit. However, for molecules whose critical diameter is close to or distinctly larger than the ZSM-5 pore size, surface modification would create a significant entropic surface barrier, and the large deposition amount for modification will lead to a higher entropic surface barrier.[50−52] Here the advantage of toluene surface permeability over ZSM-5-ASCAD suggests that although the CLD method is already recognized as an effective external surface modification method, target deposition by the ASCAD method can realize external surface modification with minimum silica deposition, which contributes to its excellent toluene mass transfer and high toluene conversion. Furthermore, the more matching reactant surface permeability over ZSM-5-ASCAD (1.72×10^{-9} for methanol and 9.09×10^{-10} for toluene, see Figure 3d) leads to an actual methanol-to-toluene ratio in the grain much closer to the feed condition, which improves methanol−toluene coconversion for PX and light olefins coproduction.

Reaction Pathway Evolution. There is a complex interaction between the reaction and diffusion in the zeolite catalysis system. On one hand, with the progress of the reaction, the resident species in the zeolite grains gradually accumulate and eventually form coke species, which causes the evolution of the diffusion properties of reactant and product molecules. Researchers used multiple techniques including pulsed field gradient nuclear magnetic resonance (PFG-NMR), the gas chromatography method, and Ab Initio Molecular Dynamics Simulation (AIMD), to track the evolution of molecular diffusion properties during the reaction on SAPO-34 molecular sieve in real-time. It was found that the intracrystalline diffusion coefficient of the product molecules decreased with the increase of the TOS.[53,54] On the other hand, the mechanism and reaction path are strongly determined by the diffusion behaviors of the reactant and product inside the zeolite-confined pores, different zeolite topologies,[55] and the change of reactant diffusion properties caused by external surface modification,[52,56,57] which will affect the catalytic performance. In this study, we tried to correlate the difference in diffusion behavior after ASCAD modification with the evolution of the reaction path and catalytic performance by an isotope labeling technique. The isotope switching experiments of methanol−toluene coreaction are carried out to investigate the change of the reaction pathways after surface modification. After feeding ^{12}C-methanol and ^{12}C-toluene for 20 min, the ^{12}C-methanol is switched to ^{13}C-methanol, and the ^{13}C-labeled products after switching are analyzed by the GC−MS. In the initial stage after isotope switching, the ^{13}C insertion speed of product ethene over modified ZSM-5-CLD and ZSM-5-ASCAD is slower than that over unmodified ZSM-5 (see Figure 4a), and even slower than propene and higher olefins (see Figure S9). This indicates that the ethene formation pathway on the external surface is inhibited after the surface modification. The ^{13}C insertion speed of propene in the initial stage after isotope switching remains unchanged after surface modification (see Figure 4b), which is similar to higher olefins (see Figure S10). For the methanol−toluene coreaction system, a large amount of toluene is fed and occupies the external surface of ZSM-5, resulting in the improvement of aromatic-based MTO reaction for ethene formation; thus, the alkene-based cycle for olefins production, especially the production of propene and higher alkenes, takes place inside the ZSM-5 grain, which is not affected by surface modification.[58] Furthermore, the higher ^{13}C contents of ethene and propene in the equilibrium stage indicate less toluene participates in light olefin production on ZSM-5-CLD than on ZSM-5 and ZSM-5-ASCAD.

On unmodified ZSM-5, PX with the ^{13}C-labeled methyl group can be generated after isotope switching via toluene methylation, toluene disproportionation, and xylene isomerization. Here, we focus on the equilibrium stage of ^{13}C contents (see Figure 4c) to investigate the reaction pathway change after surface modification. External surface reactions leading to undesired xylene distribution are banned after surface modification. Therefore, toluene can participate in only the intracrystalline reaction pathways, which provide opportunities for the insertion of ^{13}C atoms into the benzene ring, resulting in a higher ^{13}C content of aromatic products including PX (see Figures 4c and S10). The higher total ^{13}C content of PX on ZSM-5-CLD can be attributed to the lower toluene conversion and more methanol participated in PX production than on ZSM-5-ASCAD. The isotopic distributions of 5 min after ^{13}C switching provide additional evidence for the reaction pathway change after surface modification (see Figure 4d−f). The proportion of products with all carbon atoms labeled by ^{13}C (2-^{13}C labeled ethene in Figure 4d, 3-^{13}C labeled propene in Figure 4e, and 8-^{13}C labeled PX in Figure 4f) over ZSM-5-CLD is higher than that over ZSM-5 and ZSM-5-ASCAD. This indicates that the MTO reaction over ZSM-5-CLD, in which

https://doi.org/10.1021/acscatal.4c07812
ACS Catal. 2025, 15, 4147−4159

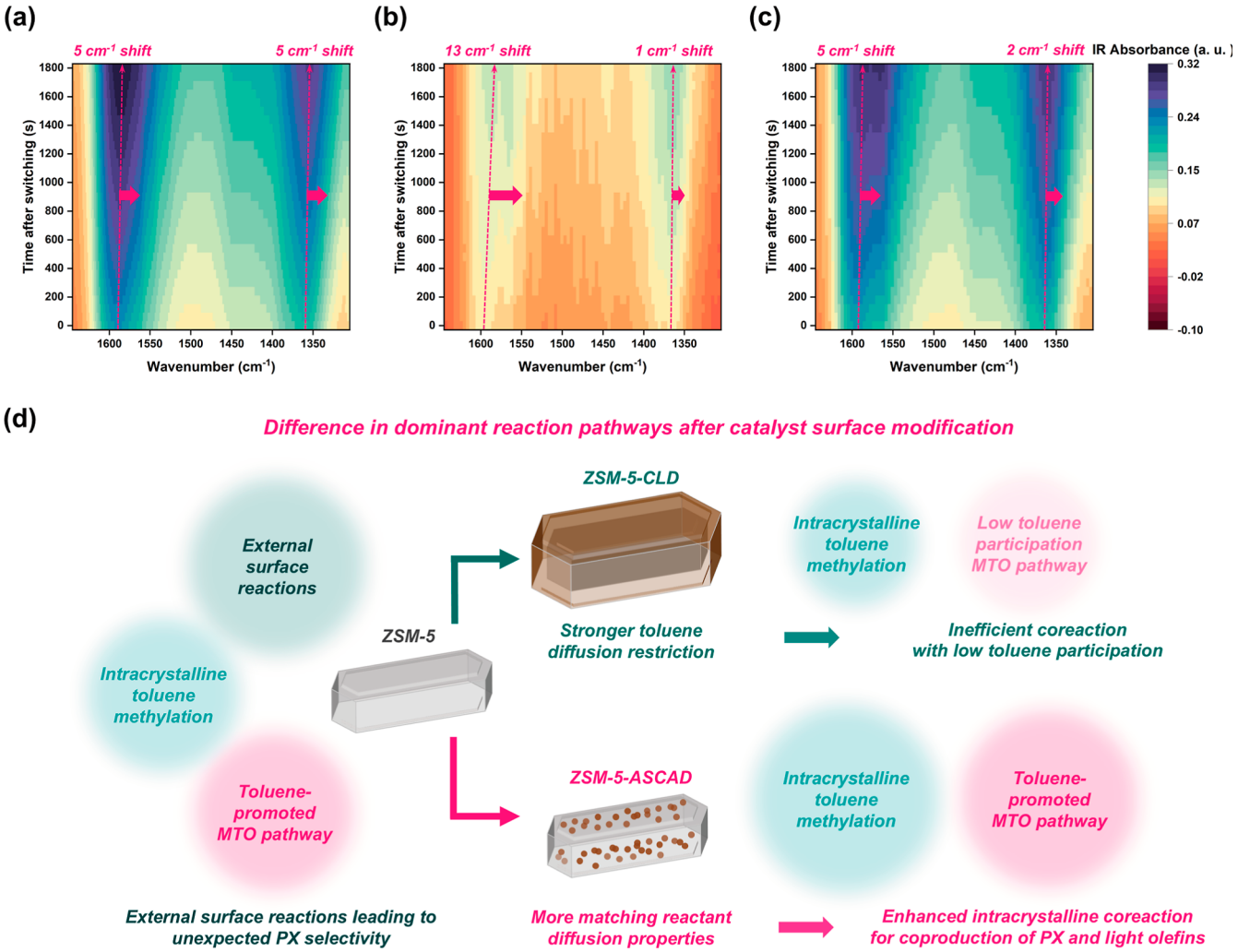

Figure 5. Dominant reaction pathways related to modification strategy. (a–c) In situ FTIR heat maps of low wavenumber region (1650–1300 cm^{-1}) recorded during isotope switching methanol–toluene coreaction over ZSM-5 (a), ZSM-5-CLD (b), and ZSM-5-ASCAD (c) under same experimental conditions. Wafers weight: 7 mg, feed ratio: $M/T = 2$, reaction temperature: 733 K, isotope switching time: 20 min on stream. (d) Schematic figure of dominant reaction pathways over ZSM-5, ZSM-5-CLD, and ZSM-5-ASCAD. Note that this figure only illustrates some of the key differences in the reaction pathways leading to the formation of dominant products.

toluene participation was depressed due to the difficulty of mass transfer over the CLD method modified ZSM-5, will account for a noticeable proportion for PX and ethene production from only methanol conversion. In contrast, for ZSM-5-ASCAD, the higher proportion of ethene with fewer ^{13}C labeled (0-^{13}C and 1-^{13}C labeled ethene in Figure 4d) over ZSM-5-ASCAD indicates that more toluene participates in the formation of ethene. In addition, the PX isotopic distribution over ZSM-5-ASCAD is similar to that over unmodified ZSM-5 except for the reduction of 1-^{13}C labeled PX and corresponding increase of the other ^{13}C-labeled PX (see Figure 4f). This suggests that the ASCAD modification has not caused significant effects on the intracrystalline PX production pathway. The proportion of 2-^{13}C to 6-^{13}C labeled PX over ZSM-5-ASCAD is higher than that over ZSM-5-CLD, which indicates an improved toluene utilization efficiency for PX production over ZSM-5-ASCAD.

In general, as shown in Figure 4g, surface modification by the ASCAD method effectively suppresses unwanted and uncontrollable external surface toluene methylation, toluene disproportionation, and xylene isomerization. Therefore, the methylation, disproportionation, and isomerization reactions are now only carried out inside the zeolite crystals, resulting in a tendency to generate para-isomers with diffusion advantages. The precise control of silica deposition has been achieved over ZSM-5-ASCAD with minimal effects on the diffusion properties of reactants and target products. The excellent toluene mass transfer ensures the occurrence of intracrystalline reaction and high toluene utilization efficiency while the more matching reactant surface permeabilities contribute to an enhanced methanol–toluene coconversion for PX and light olefins coproduction.

In situ FTIR results of ^{13}C-switching experiments of methanol–toluene coreaction further reveal the difference in dominant reaction pathways varied with surface modification of ZSM-5 (see Figures 5 and S11). Heat maps of the low wavenumber region (ν(C–C) and δ(C–H) region at 1650–1300 cm^{-1}) are given in Figure 5a–c. The absorbances at approximately 1590 cm^{-1} corresponding to the ring C–C stretching vibrations of aromatics with low substitution (including toluene, xylene, trimethylbenzene, etc.[59,60]) are slightly affected by the different aromatic distributions over the three catalysts, while the band intensity of ZSM-5-CLD is

https://doi.org/10.1021/acscatal.4c07812
ACS Catal. 2025, 15, 4147–4159

quite low compared to that of other catalysts, indicating the low aromatic introduction into this catalyst during coreaction. The maxima of the bands are fixed within 20 min on stream but red-shifted after switching to the ^{13}C-methanol and ^{12}C-toluene cofeed. This is caused by the insertion of ^{13}C atoms into the aromatic ring, and the larger shift over ZSM-5-CLD (13 cm^{-1}, see Figure 5b) than that over ZSM-5 and ZSM-5-ASCAD (5 cm^{-1}, see Figure 5a,c) indicates that more ^{13}C-atoms from methanol participates in the formation of aromatic species over ZSM-5-CLD. This provides additional evidence for the higher proportion of the MTO reaction pathway over ZSM-5-CLD. The band centered at 1365 cm^{-1} is due to the C−H bending vibrations of the substituent group of aromatic species.[61,62] Here, a more remarkable redshift (5 cm^{-1}) of this band after isotope switching is observed on ZSM-5 but only 1 cm^{-1} shift on ZSM-5-CLD and 2 cm^{-1} shift on ZSM-5-ASCAD, respectively. This indicates a more predominant occurrence of the alkylation reaction of aromatic compounds over the external surface of ZSM-5 without surface modification. Moreover, it is worth noting that the IR absorbance intensity of the low wavenumber region on ZSM-5 is significantly higher than that on ZSM-5-CLD but close to that on ZSM-5-ASCAD. This suggests that compared with ZSM-5-CLD, there are more aromatic species introduction or generation on the other two catalysts, ZSM-5 and ZSM-5-ASCAD, indicating that more toluene diffuses into the zeolite grains and reacts with methanol. The concentration of toluene within the ZSM-5-CLD grains is much lower than that of the feed, while the intracrystalline methanol to toluene molar ratio (M/T) of ZSM-5-ASCAD is similar to that of ZSM-5, facilitating the production of xylene and other aromatics. This shows that the ASCAD method has a very slight effect on molecular diffusion. This is the reason toluene can maintain high conversion over ZSM-5-ASCAD.

Based on the analysis of the difference in reaction pathways and the possibility of toluene participation in the methanol−toluene coreaction over the three catalysts, a schematic figure of the dominant reaction pathways after catalyst surface modification is given in Figure 5d. For methanol−toluene coreaction over ZSM-5, the toluene methylation pathway for xylene production and the toluene-promoted MTO pathway are dominated, while the formation of xylene isomers and some C_9^+ aromatics cannot be avoided due to the external acid catalysis. After surface modification, the external surface reactions are inhibited, and the intracrystalline toluene methylation pathway mainly produces PX under the shape-selective effect of the zeolite. Methanol−toluene coconversion on zeolite modified by the two deposition methods is different in the dominant reaction pathways. The thick silica deposition layer of ZSM-5-CLD leads to a strong diffusion restriction on reactant toluene and a low toluene concentration within the grain, which further results in an MTO reaction pathway with low toluene participation. In contrast, the ASCAD method achieves a targeted deposition of silica at the external surface acid sites and more matching reactant diffusion properties leading to a similar intracrystalline M/T ratio to the ZSM-5, which further results in an enhanced toluene-promoted MTO pathway for PX and ethene coproduction dominating over ZSM-5-ASCAD. The excellent catalytic performance presented by ZSM-5-ASCAD can be summarized in combination with the above analysis of the acid properties and the diffusion properties of reactants and products after modification. First, the effective coverage of the external surface acidic sites and the enhancement of the PX diffusion lead to the ultrahigh product selectivity of PX. Second, the excellent toluene mass transfer ensures high toluene utilization efficiency. Third, the more matching reactant (methanol and toluene) diffusion properties lead to enhanced methanol−toluene coconversion for PX and light olefins coproduction.

CONCLUSIONS

In conclusion, ZSM-5 is modified by the ASCAD method, which precisely controls the deposition of silica over the external surface of ZSM-5. The ZSM-5-ASCAD achieves targeted coverage of the external surface acid sites and presents a high performance in methanol−toluene coconversion. After catalyst modification, the unrestricted methylation, disproportionation, and isomerization of aromatics, which are dominant on the external surface of unmodified ZSM-5, have been inhibited, and the coreaction of methanol−toluene in the internal channel for the coproduction of PX and ethene has been enhanced. The improvement of mass transfer of reactant toluene and target product PX, and more matching reactant diffusion properties for methanol−toluene coconversion over ZSM-5-ASCAD, together contribute to the excellent catalytic performance. As a result, at atmospheric pressure, 733 K, WHSV = 2 h^{-1}, and methanol/toluene = 2 (molar ratio), the ZSM-5-ASCAD catalyst exhibits an ultrahigh PX selectivity (among xylenes, 99.5%) and outstanding toluene conversion (43%), together with an excellent target product selectivity in methanol−toluene coreaction (94% for PX and light olefins among all hydrocarbon products). This work provides a precise and efficient modification approach to prepare catalysts with high selectivity and high reactivity at the same time. The application of this target modification strategy for ZSM-5 and the coreaction reaction system enables the joint production of value-added aromatic products and light olefins. By suppressing the acidity on the external surface and confining the reaction within the channel of zeolite with shape-selective properties, highly shape-selective zeolite acid catalysis has been achieved, which provides an effective strategy for further improving the catalytic performance of the zeolite-catalyzed process.

ASSOCIATED CONTENT

Supporting Information

The Supporting Information is available free of charge at https://pubs.acs.org/doi/10.1021/acscatal.4c07812.

Experimental procedures; SEM images; XRD pattern; STEM images of the FIB cross section and TEM images; comparison of the catalytic performance; IR spectra after DTBPy adsorption and desorption; ZLC desorption curves; multiple-crystal IR spectra measured using IRM; multiple-crystal reactant uptakes; ^{13}C contents after ^{12}C/^{13}C-methanol switching; in situ FTIR spectra; structural properties; NH_3-TPD results; catalyst tests with ASCAD cycles; catalyst tests with CVD cycles; catalytic performance; and comparison with catalysts in previous reports (PDF)

AUTHOR INFORMATION

Corresponding Authors

Jingfeng Han − *National Engineering Research Center of Lower-Carbon Catalysis Technology, Dalian Institute of Chemical Physics, Chinese Academy of Sciences, Dalian 116023, China*; Email: jfhan@dicp.ac.cn

Zhongmin Liu − *National Engineering Research Center of Lower-Carbon Catalysis Technology, Dalian Institute of*

https://doi.org/10.1021/acscatal.4c07812
ACS Catal. 2025, 15, 4147−4159

Chemical Physics and State Key Laboratory of Catalysis, Dalian Institute of Chemical Physics, Chinese Academy of Sciences, Dalian 116023, China; orcid.org/0000-0002-7999-2940; Email: liuzm@dicp.ac.cn

Authors

Yimo Wu − *National Engineering Research Center of Lower-Carbon Catalysis Technology, Dalian Institute of Chemical Physics, Chinese Academy of Sciences, Dalian 116023, China; University of Chinese Academy of Sciences, Beijing 100049, China;* orcid.org/0000-0002-7319-8260

Nan Wang − *National Engineering Research Center of Lower-Carbon Catalysis Technology, Dalian Institute of Chemical Physics, Chinese Academy of Sciences, Dalian 116023, China*

Enze Chen − *National Engineering Research Center of Lower-Carbon Catalysis Technology, Dalian Institute of Chemical Physics, Chinese Academy of Sciences, Dalian 116023, China; University of Chinese Academy of Sciences, Beijing 100049, China*

Haohao Feng − *National Engineering Research Center of Lower-Carbon Catalysis Technology, Dalian Institute of Chemical Physics, Chinese Academy of Sciences, Dalian 116023, China; University of Chinese Academy of Sciences, Beijing 100049, China*

Dong Fan − *National Engineering Research Center of Lower-Carbon Catalysis Technology, Dalian Institute of Chemical Physics, Chinese Academy of Sciences, Dalian 116023, China;* orcid.org/0000-0002-8815-0163

Yang Yu − *Division of Energy Research Resources, Dalian Institute of Chemical Physics, Chinese Academy of Sciences, Dalian 116023, China*

Li Wang − *Division of Energy Research Resources, Dalian Institute of Chemical Physics, Chinese Academy of Sciences, Dalian 116023, China*

Te Ji − *Shanghai Synchrotron Radiation Facility, Shanghai Advanced Research Institute, Chinese Academy of Sciences, Shanghai 201210, China*

Zhengxi Yu − *National Engineering Research Center of Lower-Carbon Catalysis Technology, Dalian Institute of Chemical Physics, Chinese Academy of Sciences, Dalian 116023, China*

Yingxu Wei − *National Engineering Research Center of Lower-Carbon Catalysis Technology, Dalian Institute of Chemical Physics, Chinese Academy of Sciences, Dalian 116023, China;* orcid.org/0000-0002-0412-1980

Complete contact information is available at: https://pubs.acs.org/10.1021/acscatal.4c07812

Notes

The authors declare no competing financial interest.

■ ACKNOWLEDGMENTS

We thank the National Natural Science Foundation of China (22288101, 21991093, 21991092, 21991090, 22172166), the Youth Innovation Promotion Association CAS (2021182), the Clean Combustion and Low-carbon Utilization of Coal, Strategic Priority Research Program of the Chinese Academy of Sciences (grant no. XDA 29000000), the Innovation Research Foundation of Dalian Institute of Chemical Physics, Chinese Academy of Sciences (DICP I202217) for the financial support. We thank the SSRF (BL06B) beamline for experimental data collection.

■ REFERENCES

(1) Tomás, R. A. F.; Bordado, J. C. M.; Gomes, J. F. P. p-Xylene Oxidation to Terephthalic Acid: A Literature Review Oriented toward Process Optimization and Development. *Chem. Rev.* **2013**, *113* (10), 7421−7469.

(2) Kumar, L.; Asthana, S.; Newalkar, B. L.; Pant, K. K. Selective toluene methylation to p-xylene: current status & future perspective. *Catal. Rev.* **2022**, *66*, 820.

(3) Wu, Y.; Han, J.; Zhang, W.; Yu, Z.; Wang, K.; Fang, X.; Wei, Y.; Liu, Z. Combined Strategies Enable Highly Selective Light Olefins and para-Xylene Production on Single Catalyst Bed. *J. Am. Chem. Soc.* **2024**, *146* (12), 8086−8097.

(4) Zhang, W.; Lin, S.; Wei, Y.; Tian, P.; Ye, M.; Liu, Z. Cavity-controlled methanol conversion over zeolite catalysts. *Natl. Sci. Rev.* **2023**, *10* (9), nwad120.

(5) Huang, X.; Wang, R. Z.; Pan, X.; Wang, C. F.; Fan, M. H.; Zhu, Y. F.; Wang, Y. G.; Peng, J. Catalyst design strategies towards highly shape-selective HZSM-5 for paraxylene through toluene alkylation. *Green Energy Environ.* **2020**, *5* (4), 385−393.

(6) Kim, J.-H.; Ishida, A.; Okajima, M.; Niwa, M. Modification of HZSM-5 by CVD of Various Silicon Compounds and Generation of Para-Selectivity. *J. Catal.* **1996**, *161* (1), 387−392.

(7) Weber, R. W.; Möller, K. P.; O'Connor, C. T. The chemical vapour and liquid deposition of tetraethoxysilane on ZSM-5, mordenite and beta. *Microporous Mesoporous Mater.* **2000**, *35*−*36*, 533−543.

(8) Manstein, H.; Möller, K. P.; Böhringer, W.; O'Connor, C. T. Effect of the deposition temperature on the chemical vapour deposition of tetraethoxysilane on ZSM-5. *Microporous Mesoporous Mater.* **2002**, *51* (1), 35−42.

(9) Zhu, Z.; Xie, Z.; Chen, Q.; Kong, D.; Li, W.; Yang, W.; Li, C. Chemical liquid deposition with polysiloxane of ZSM-5 and its effect on acidity and catalytic properties. *Microporous Mesoporous Mater.* **2007**, *101* (1), 169−175.

(10) Teng, H.; Wang, J.; Ren, X.; Chen, D. Disproportionation of Toluene by Modified ZSM-5 Zeolite Catalysts with High Shape-selectivity Prepared Using Chemical Liquid Deposition with Tetraethyl Orthosilicate. *Chin. J. Chem. Eng.* **2011**, *19* (2), 292−298.

(11) Ahn, J. H.; Kolvenbach, R.; Al-Khattaf, S. S.; Jentys, A.; Lercher, J. A. Enhancing shape selectivity without loss of activity - novel mesostructured ZSM5 catalysts for methylation of toluene to p-xylene. *Chem. Commun.* **2013**, *49* (90), 10584−10586.

(12) Lu, P.; Fei, Z. Y.; Li, L.; Feng, X. Z.; Ji, W. J.; Ding, W. P.; Chen, Y.; Yang, W. M.; Xie, Z. K. Effects of controlled SiO2 deposition and phosphorus and nickel doping on surface acidity and diffusivity of medium and small sized HZSM-5 for para-selective alkylation of toluene by methanol. *Appl. Catal., A* **2013**, *453*, 302−309.

(13) Zhang, J. G.; Qian, W. Z.; Kong, C. Y.; Wei, F. Increasing para-Xylene Selectivity in Making Aromatics from Methanol with a Surface-Modified Zn/P/ZSM-5 Catalyst. *ACS Catal.* **2015**, *5* (5), 2982−2988.

(14) Han, H.; Yang, H.; Zhang, A. F.; Ren, L. M.; Nie, X. W.; Chen, C. Q.; Liu, M.; Shi, C. A.; Song, C. S.; Guo, X. W. Design of highly stable metal/ZSM-5 catalysts for the shape-selective alkylation of toluene with methanol to para-xylene. *Inorg. Chem. Front.* **2022**, *9* (13), 3348−3358.

(15) Van Vu, D.; Miyamoto, M.; Nishiyama, N.; Egashira, Y.; Ueyama, K. Selective formation of para-xylene over H-ZSM-5 coated with polycrystalline silicalite crystals. *J. Catal.* **2006**, *243* (2), 389−394.

(16) Wang, C. F.; Zhang, L.; Huang, X.; Zhu, Y. F.; Li, G.; Gu, Q. F.; Chen, J. Y.; Ma, L. G.; Li, X. J.; He, Q. H.; Xu, J. B.; Sun, Q.; Song, C. Q.; Peng, M.; Sun, J. L.; Ma, D. Maximizing sinusoidal channels of HZSM-5 for high shape-selectivity to p-xylene. *Nat. Commun.* **2019**, *10*, 4348.

(17) Zheng, S.; Heydenrych, H. R.; Jentys, A.; Lercher, J. A. Influence of Surface Modification on the Acid Site Distribution of HZSM-5. *J. Phys. Chem. B* **2002**, *106* (37), 9552−9558.

(18) Kaur, H.; Chaudhary, S.; Kaur, H.; Chaudhary, M.; Jena, K. C. Hydrolysis and Condensation of Tetraethyl Orthosilicate at the Air−Aqueous Interface: Implications for Silica Nanoparticle Formation. *ACS Appl. Nano* **2022**, *5* (1), 411−422.

(19) Ristanovic, Z.; Hofmann, J. P.; Deka, U.; Schuelli, T. U.; Rohnke, M.; Beale, A. M.; Weckhuysen, B. M. Intergrowth Structure and

Aluminium Zoning of a Zeolite ZSM-5 Crystal as Resolved by Synchrotron-Based Micro X-Ray Diffraction Imaging. *Angew. Chem., Int. Ed.* **2013**, *52* (50), 13382−13386.
(20) Hofmann, J. P.; Rohnke, M.; Weckhuysen, B. M. Recent advances in secondary ion mass spectrometry of solid acid catalysts: large zeolite crystals under bombardment. *Phys. Chem. Chem. Phys.* **2014**, *16* (12), 5465−5474.
(21) Sun, X.; Mueller, S.; Shi, H.; Haller, G. L.; Sanchez-Sanchez, M.; van Veen, A. C.; Lercher, J. A. On the impact of co-feeding aromatics and olefins for the methanol-to-olefins reaction on HZSM-5. *J. Catal.* **2014**, *314*, 21−31.
(22) Shi, Q.; Gonçalves, J. C.; Ferreira, A. F. P.; Rodrigues, A. E. A review of advances in production and separation of xylene isomers. *Chem. Eng. Process.* **2021**, *169*, 108603.
(23) Phatanasri, S.; Praserthdam, P.; Punsupsawat, T. Influence of Fe or Zn Loading Method on Toluene Methylation over MFI-Type Zeolite Catalysts. *Korean J. Chem. Eng.* **2000**, *17* (4), 414.
(24) Aboul-Gheit, A. K.; Aboul-Enein, A. A.; Awadallah, A. E.; Ghoneim, S. A.; Emam, E. A. Para-Xylene Maximization Part VIII: Promotion of H-ZSM-5 Zeolite by Pt and HF Doping for Use as Catalysts in Toluene Alkylation with Methanol. *Chin. J. Catal.* **2010**, *31* (10), 1209.
(25) Yi, D.; Meng, X.; Xu, X.; Liu, N.; Shi, L. Catalytic Performance of Modified ZSM-5 Designed with Selectively Passivated External Surface Acidity by Phosphorus. *Ind. Eng. Chem. Res.* **2019**, *58* (24), 10154.
(26) Miyamoto, M.; Kamei, T.; Nishiyama, N.; Egashira, Y.; Ueyama, K. Single Crystals of ZSM-5/Silicalite Composites. *Adv. Mater.* **2005**, *36* (44), 1985.
(27) Sotelo, J. L.; Uguina, M. A.; Valverde, J. L.; Serrano, D. P. Deactivation of Toluene Alkylation with Methanol over Magnesium-Modified ZSM-5 Shape Selectivity Changes Induced by Coke Formation. *Appl. Catal., A* **1994**, *114* (2), 273.
(28) Cavallaro, S.; Pino, L.; Tsiakaras, P.; Giordano, N.; Rao, B. S. Alkylation of Toluene with Methanol III: Para-Selectivity on Modified ZSM-5 Zeolites. *Zeolites* **1987**, *7* (5), 408.
(29) Li, G.; Wu, C.; Ji, D.; Dong, P.; Zhang, Y.; Yang, Y. Acidity and Catalyst Performance of Two Shape-Selective HZSM-5 Catalysts for Alkylation of Toluene with Methanol. *React. Kinet., Mech. Catal.* **2020**, *129* (2), 963.
(30) Zhao, Y.; Tan, W.; Wu, H.; Zhang, A.; Liu, M.; Li, G.; Wang, X.; Song, C.; Guo, X. Effect of Pt on Stability of Nano-Scale ZSM-5 Catalyst for Toluene Alkylation with Methanol into p-Xylene. *Catal. Today* **2011**, *160* (1), 179.
(31) Young, L. B.; Butter, S. A.; Kaeding, W. W. Shape Selective Reactions with Zeolite Catalysts. III. Selectivity in Xylene Isomerization, Toluene-Methanol Alkylation, and Toluene Disproportionation over ZSM-5 Zeolite Catalysts. *J. Catal.* **1982**, *76* (2), 418.
(32) Janardhan, H. L.; Shanbhag, G. V.; Halgeri, A. B. Shape-Selective Catalysis by Phosphate Modified ZSM-5: Generation of New Acid Sites with Pore Narrowing. *Appl. Catal., A* **2014**, *471*, 12.
(33) Wang, Y.; Liu, M.; Zhang, A.; Zuo, Y.; Ding, F.; Chang, Y.; Song, C.; Guo, X. Methanol Usage in Toluene Methylation over Pt Modified ZSM-5 Catalyst: Effects of Total Pressure and Carrier Gas. *Ind. Eng. Chem. Res.* **2017**, *56* (16), 4709.
(34) Zhou, J.; Wang, Y.; Zou, W.; Wang, C.; Li, L.; Liu, Z.; Zheng, A.; Kong, D.; Yang, W.; Xie, Z. Mass Transfer Advantage of Hierarchical Zeolites Promotes Methanol Converting into Para-Methyl Group in Toluene Methylation. *Ind. Eng. Chem. Res.* **2017**, *56* (33), 9310.
(35) Tan, W.; Liu, M.; Zhao, Y.; Hou, K.; Wu, H.; Zhang, A.; Liu, H.; Wang, Y.; Song, C.; Guo, X. Para-Selective Methylation of Toluene with Methanol over Nano-Sized ZSM-5 Catalysts: Synergistic Effects of Surface Modifications with SiO2, P2O5 and MgO. *Microporous Mesoporous Mater.* **2014**, *196*, 18.
(36) Hibino, T.; Niwa, M.; Murakami, Y. Shape-selectivity over hzsm-5 modified by chemical vapor deposition of silicon alkoxide. *J. Catal.* **1991**, *128* (2), 551−558.
(37) Breen, J.; Burch, R.; Kulkarni, M.; Collier, P.; Golunski, S. Enhanced Para-Xylene Selectivity in the Toluene Alkylation Reaction at Ultralow Contact Time. *J. Am. Chem. Soc.* **2005**, *127* (14), 5020.
(38) McIntyre, J. E. The Historical Development of Polyesters. In *Modern Polyesters: Chemistry and Technology of Polyesters and Copolyesters*; Wiley, 2004; pp 1−28.
(39) Armaroli, T.; Bevilacqua, M.; Trombetta, M.; Alejandre, A. d. G.; Ramirez, J.; Busca, G. An FT-IR study of the adsorption of aromatic hydrocarbons and of 2,6-lutidine on H-FER and H-ZSM-5 zeolites. *Appl. Catal., A* **2001**, *220* (1), 181−190.
(40) Ungureanu, A.; Hoang, T. V.; Trong On, D.; Dumitriu, E.; Kaliaguine, S. An investigation of the acid properties of UL-ZSM-5 by FTIR of adsorbed 2,6-ditertbutylpyridine and aromatic transalkylation test reaction. *Appl. Catal., A* **2005**, *294* (1), 92−105.
(41) Gora-Marek, K.; Tarach, K.; Choi, M. 2,6-Di-tert-butylpyridine Sorption Approach to Quantify the External Acidity in Hierarchical Zeolites. *J. Phys. Chem. C* **2014**, *118* (23), 12266−12274.
(42) Morterra, C.; Cerrato, G.; Meligrana, G. Revisiting the Use of 2,6-Dimethylpyridine Adsorption as a Probe for the Acidic Properties of Metal Oxides. *Langmuir* **2001**, *17* (22), 7053−7060.
(43) Lin, S.; Zhi, Y.; Liu, Z.; Yuan, J.; Liu, W.; Zhang, W.; Xu, Z.; Zheng, A.; Wei, Y.; Liu, Z. Multiscale dynamical cross-talk in zeolite-catalyzed methanol and dimethyl ether conversions. *Natl. Sci. Rev.* **2022**, *9* (9), nwac151.
(44) Li, J.; Ji, W.; Liu, M.; Zhao, G.; Jia, W.; Zhu, Z. New insight into the alkylation-efficiency of methanol with toluene over ZSM-5: Microporous diffusibility significantly affects reacting-pathways. *Microporous Mesoporous Mater.* **2019**, *282*, 252−259.
(45) Chen, Q. T.; Liu, J.; Yang, B. Identifying the key steps determining the selectivity of toluene methylation with methanol over HZSM-5. *Nat. Commun.* **2021**, *12* (1), 3725.
(46) Bonilla, M. R.; Titze, T.; Schmidt, F.; Mehlhorn, D.; Chmelik, C.; Valiullin, R.; Bhatia, S. K.; Kaskel, S.; Ryoo, R.; Kärger, J. Diffusion Study by IR Micro-Imaging of Molecular Uptake and Release on Mesoporous Zeolites of Structure Type CHA and LTA. *Materials* **2013**, *6* (7), 2662−2688.
(47) Kärger, J.; Binder, T.; Chmelik, C.; Hibbe, F.; Krautscheid, H.; Krishna, R.; Weitkamp, J. Microimaging of transient guest profiles to monitor mass transfer in nanoporous materials. *Nat. Mater.* **2014**, *13* (4), 333−343.
(48) Mirth, G.; Lercher, J. A. COADSORPTION OF TOLUENE AND METHANOL ON HZSM-5 ZEOLITES. *J. Phys. Chem.* **1991**, *95* (9), 3736−3740.
(49) Zheng, S.; Jentys, A.; Lercher, J. A. Xylene isomerization with surface-modified HZSM-5 zeolite catalysts: An in situ IR study. *J. Catal.* **2006**, *241* (2), 304−311.
(50) Remi, J. C. S.; Lauerer, A.; Chmelik, C.; Vandendael, I.; Terryn, H.; Baron, G. V.; Denayer, J. F. M.; Kärger, J. The role of crystal diversity in understanding mass transfer in nanoporous materials. *Nat. Mater.* **2016**, *15* (4), 401−406.
(51) Gobin, O. C.; Reitmeier, S. J.; Jentys, A.; Lercher, J. A. Role of the Surface Modification on the Transport of Hexane Isomers in ZSM-5. *J. Phys. Chem. C* **2011**, *115* (4), 1171−1179.
(52) Chen, J. X.; Hu, S.; Chen, Z.; Sun, X. C.; Chen, M. H.; Chen, T. J.; Ye, G. H.; Zhou, X. G. SiO2 Deposition to Regulate Surface Barriers and Its Impact on ZSM-5 Catalyzed Reactions with Distinct Molecular Sizes. *Catal. Lett.* **2023**, *153* (8), 2504−2516.
(53) Han, J.; Liu, Z.; Li, H.; Zhong, J.; Zhang, W.; Huang, J.; Zheng, A.; Wei, Y.; Liu, Z. Simultaneous Evaluation of Reaction and Diffusion over Molecular Sieves for Shape-Selective Catalysis. *ACS Catal.* **2020**, *10* (15), 8727−8735.
(54) Gao, S.; Xu, S.; Wei, Y.; Qiao, Q.; Xu, Z.; Wu, X.; Zhang, M.; He, Y.; Xu, S.; Liu, Z. Insight into the deactivation mode of methanol-to-olefins conversion over SAPO-34: Coke, diffusion, and acidic site accessibility. *J. Catal.* **2018**, *367*, 306−314.
(55) Liu, Z.; Chu, Y.; Tang, X.; Huang, L.; Li, G.; Yi, X.; Zheng, A. Diffusion Dependence of the Dual-Cycle Mechanism for MTO Reaction Inside ZSM-12 and ZSM-22 Zeolites. *J. Phys. Chem. C* **2017**, *121* (41), 22872−22882.
(56) Yang, Q.; Li, Y.; Chen, Z.; Hu, L.; Li, Z.; Wang, Y.; Zhao, Z.; Xu, C.; Jiang, G. Core-shell structured HZSM-5@$_2$ catalysts with tunable

https://doi.org/10.1021/acscatal.4c07812
ACS Catal. 2025, 15, 4147−4159

shell thickness for efficient *n*-butane catalytic cracking. *AlChE J.* **2021**, *67* (4), No. e17130.
(57) Hu, S.; Liu, J.; Ye, G.; Zhou, X.; Coppens, M.-O.; Yuan, W. Effect of External Surface Diffusion Barriers on Platinum/Beta-Catalyzed Isomerization of n-Pentane. *Angew. Chem., Int. Ed.* **2021**, *60* (26), 14394−14398.
(58) Li, J.; Wang, Y.; Jia, W.; Xi, Z.; Chen, H.; Zhu, Z.; Hu, Z. Effect of external surface of HZSM-5 zeolite on product distribution in the conversion of methanol to hydrocarbons. *J. Energy Chem.* **2014**, *23* (6), 771−780.
(59) Mirth, G.; Lercher, J. A. INSITU IR SPECTROSCOPIC STUDY OF THE SURFACE SPECIES DURING METHYLATION OF TOLUENE OVER HZSM-5. *J. Catal.* **1991**, *132* (1), 244−252.
(60) Uslamin, E. A.; Saito, H.; Kosinov, N.; Pidko, E.; Sekine, Y.; Hensen, E. J. M. Aromatization of ethylene over zeolite-based catalysts. *Catal. Sci. Technol.* **2020**, *10* (9), 2774−2785.
(61) Castaño, P.; Elordi, G.; Olazar, M.; Aguayo, A. T.; Pawelec, B.; Bilbao, J. Insights into the coke deposited on HZSM-5, Hβ and HY zeolites during the cracking of polyethylene. *Appl. Catal., B* **2011**, *104* (1), 91−100.
(62) Park, G.; Kang, J.; Park, S.-J.; Kim, Y. T.; Kwak, G.; Kim, S. Effect of acid modification of ZSM-5 catalyst on performance and coke formation for methanol-to-hydrocarbon reaction. *Mol. Catal.* **2022**, *531*, 112702.

https://doi.org/10.1021/acscatal.4c07812
ACS Catal. 2025, 15, 4147−4159